MZUZU UNIVERSITY

A STUDY OF THERMOLUMINESCENCE OF PEAK I IN α-Al_2O_3:C : A COMPUTER SIMULATION APPROACH

BY

CHISOMO GADAMA (BSPHEH0322)

A project submitted to the Department of Physics and Electronics, Faculty of Science, Technology, and Innovation, Mzuzu University, in partial fulfillment of the requirements of the degree of Bachelors of Science (Honours) in Physics and Electronics

January, 2024

Declaration

I, **Chisomo Gadama**, do hereby declare that this work is original and has not been submitted for any other degree award to any other university before.

Student's signature..... Date...../...../.....

This dissertation was submitted with the approval of the following supervisor:

Dr. A. Nyirenda,

Department of Physics and Electronics,

Mzuzu University.

Sign.....Date...../...../.....

Dedication

This piece of work is dedicated to my parents, Mr and Mrs Gadama, for their love, allowing me to pursue honours degree when I asked and the help rendered throughout my study. I am always proud to have you and surely appreciate your hard work; may the Almighty God continue blessing you.

Acknowledgment

First and foremost, I thank God the Almighty Lord for the gift of life, blessings and protection during my studies. You were a pillar of strength, hope and energy that charge me on.

I also extend my gratitude to my supervisor, Dr A. Nyirenda, for giving me this rare opportunity to conduct research under his supervision. I would also like to thank him for his support, enthusiasm in talking, teaching, and guiding me on what I was supposed to do, for his readiness and willngness in answering my emails or otherwise during my one-year stay at Mzuzu University. God bless you Dr A. Nyirenda and your family. A lot of thanks to all the staff members in the department of Physics and Electronics at Mzuzu University, so numerous to mention, and my fellow BSPHEH students for making my stay at Mzuzu University easy and memorable. I won't forget you folks.

Finally, I acknowledge my parents Mr and Mrs Gadama for their encouragement and support during my studies and this project work. I convey my deepest gratitude to you all. Be blessed.

When I am working on a problem I never think about beauty. I only think about how to solve the problem. But when I have finished, if the solution is not beautiful, I know it is wrong - Buckminster Fuller

Abstract

This work explores the thermoluminescence properties of Peak I in α-Al_2O_3: C. The study employs the OTOR model to simulate the thermoluminescent behavior of Peak I, for both irradiation and readout stages, using the Mathematica software. The simulation results show that (i) the concentration of holes and electrons in the valence band and conduction band respectively, increases with irradiation time and saturates for irradiation times longer that 10 s (10^{17} Gray) for the total electron trap concentration (N) of 10^{15}; (ii) the maximum peak intensity decreases with increasing heating rate; (iii) the maximum peak position shifts towards higher temperatures with increasing heating rate; (iv) the FWHM increases with increasing heating rate; (v) the FWHM, the peak position and the geometrical factor ,μ, are all independent of the irradiation dose; and (vi) the maximum peak intensity increases with increasing irradiation dose. Thus, the TL of Peak I in α-Al_2O_3: C follows first-order kinetics.

Keywords: Thermoluminescence, Irradiation Stage, Readout Stage, Heating rate, Maximum peak intensity, Maximum peak position.

Table of contents

List of Figures

List of Tables

Chapter 1

Introduction

This chapter covers background information, Problem statement, objectives, and significance of the study.

1.1 Background information

When an insulating crystal is exposed to ionizing radiation, free electrons and holes are generated. Some of these holes and electrons are trapped in defects in the crystal lattices of the solid. Heating such a pre-irradiated solid may cause the removal of electrons from their traps, which subsequently recombine with holes at recombination centers giving off light. This phenomenon is called as thermoluminescence (TL). The curve plotted versus temperature is called as TL glow curve. The shape and position of the resultant TL glow curves can be analyzed to extract information on the various kinetic parameters of the trapping process; trap depth, frequency factor, trapping and retrapping rates, kinetic order and etc[1].

TL requires that a material must be an insulator or a semiconductor and must have been previously exposed to an radiation source such as beta or gamma irradiation before being heated at a controlled rate to produce luminescence [2]. The TL technique is used to study point defects involved in luminescence of α-Al_2O_3. A glow curve of α-Al_2O_3, generally, shows three peaks; the main dosimetric peak of high intensity (peak II) and the other two peaks of lower intensity called secondary glow peaks (peaks I and III). The research contributes to a better understanding of the material's luminescent properties and may have implications for the development of advanced thermoluminescent materials with enhanced performance.

1.2 Problem Statement

Several scholars[2, 3, 4] have conducted studies that the major focus on α-$Al_2O_3 : C$ has been on the main peak also referred to as the dosimetric peak. The studies in the main peak have included both experimental and computer simulation approaches. However, the studies of secondary peaks in the material have focused only on the experimental behaviour. The current study aims to address this gap by employing simulation techniques to explore the dynamics and characteristics of peak I. By undertaking this research, we aim to add important ideas to the field and improve our understanding of the detailed aspects connected to Peak I, thus complementing the existing body of experimental knowledge.

1.3 Main Objective

The main objective was to study the TL behavior of secondary peak I in α-$Al_2O_3 : C$ using a computer simulation approach.

1.4 Significance of the study

- The study aims at contributing to a better understanding of the thermoluminescent properties of carbon-doped aluminum oxide on the dynamics of TL phenomena.

- By simulating the secondary peak, the study serves to validate and corroborate experimental findings, enhancing the reliability of the observed thermoluminescent behavior particularly concerning the secondary peak. This knowledge is valuable for materials science offering a deeper understanding of the traps and the processes responsible for TL in the material.

Chapter 2

Theoretical background

This chapter provides the available theory related to the study of thermoluminescence of peak I in α-Al_2O_3:C.

2.1 Luminescence

Luminescence is the emission of light by a material as a consequence of absorption of energy [5, 6]. A material that emits light is called a luminescent material. More precisely, luminescence is produced by the selective excitation of the atomic or molecular energy levels. The atom or the molecule is taken to a higher energy state because of excitation and its fall to ground state results in the emission of light, which is called luminescence. There are different sources of excitation, namely, ultraviolet (UV) light, x-rays, γ-rays, etc. For instance, some minerals show some kind of luminescence under ultra-violet light exposure and some need x-ray bombardment. The presence of atomic centers whose energy levels are protected from the thermal vibrations of the atoms of the bulk medium, for example, the transitions of inner $4f$ electrons in lanthanide rare-earth ions [7], is the specific characteristic which provides an inorganic solid the luminescent property. Luminescence phenomena can also be observed in organic solids. While the luminescence of inorganic solids is mostly due to impurity atoms or other lattice defects, the luminescence in organic solids is attributed to molecular complexes [8]. After the absorption of radiation, the emission of light takes place in a characteristic time t, and this parameter allows us to sub-classify the process of luminescence. Conventionally, emissions with decay time shorter than 10^{-8} s are referred to as fluorescence, and those with decay time greater than that are known as phosphorescence [9]. This phenomenon is shown in Figure 2.1. While fluorescence takes place simultaneously with the absorption of radiation and stops immediately when the radiation ceases,

phosphorescence continues to be observed after the excitation has been removed. In other words, phosphorescence takes place under the involvement of some metastable state M, which is an energy level from which transitions to any lower energy levels are forbidden [1]. Thus, the luminescence that occurs after an electron is brought to a metastable state as a result of the excitation of the system is called phosphorescence. If a system brought to its metastable state is completely unperturbed, then it would remain in such a state for a relatively long period. Absorption transition from the ground state (G) to M is also forbidden, though it can be reached indirectly as shown in Figure 2.2

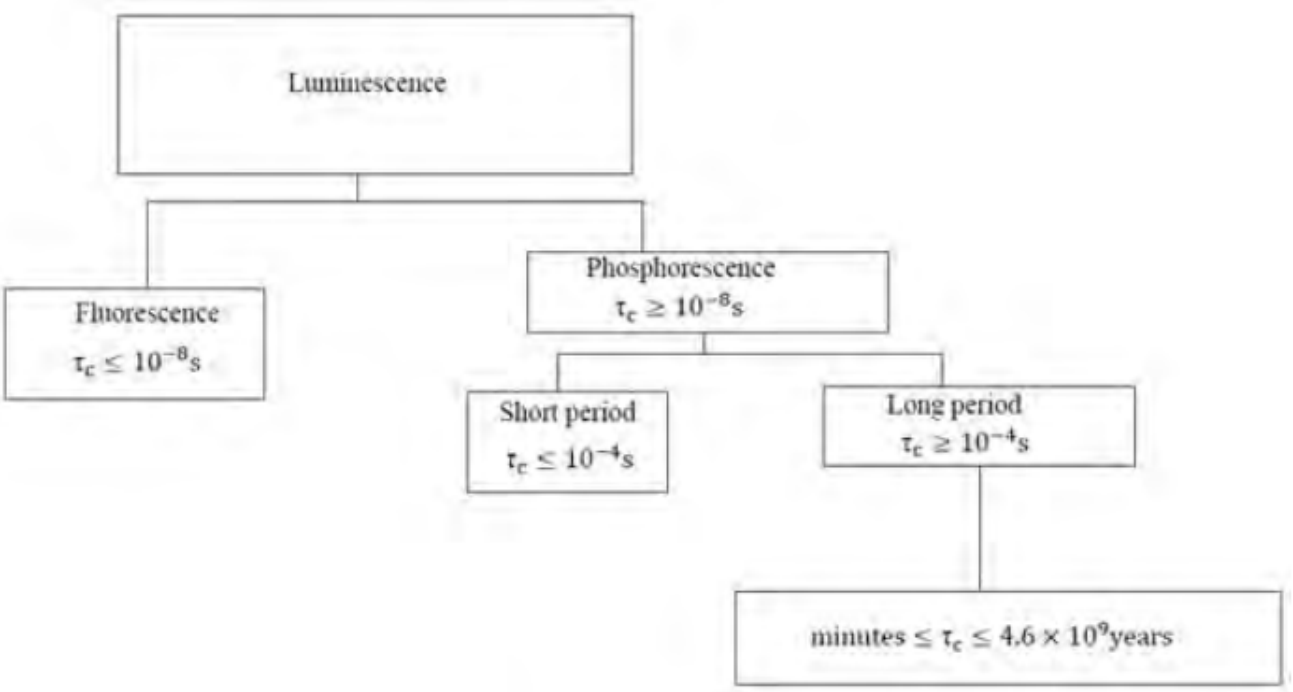

Figure 2.1: The types of luminescence based on the characteristic time t for the emission of light to take place [5]

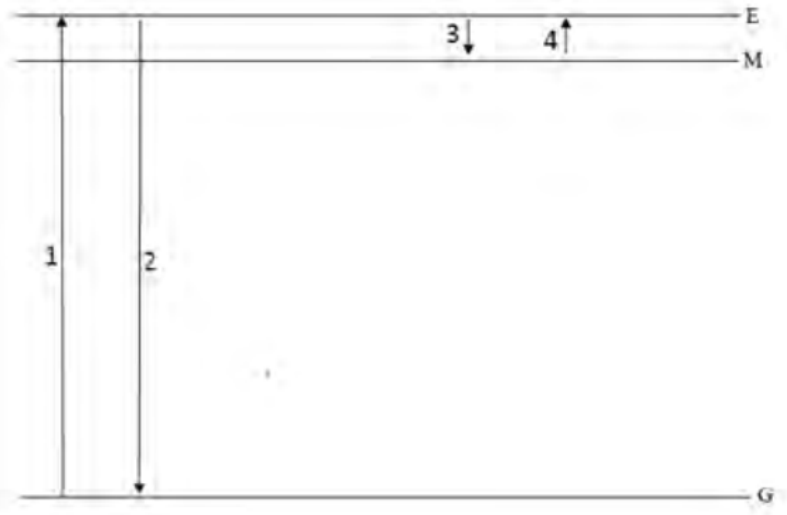

Figure 2.2: Energy level diagram illustrating (1) excitation, (2) emission, (3) falling to metastable state, and (4) depopulation of the metastable state

For example, after an electron has attained the state E as a result of excitation shown by transition 1, it can fall to M (transition 2). Consider the conditions that M is separated from E by a small energy gap and the system is in thermal equilibrium with its surrounding medium. Under such cases, the electron can return to state E following depopulation of the state M upon the application of some thermal energy. From there, transitions can take place as described in the case of fluorescence (transition 2). Therefore, phosphorescence spectrum contains emissions which are also present in fluorescence. Since the emission intensity changes with even small changes in temperature, phosphorescence is sensitive to changes in temperature in contrast to fluorescence.

To describe light-emitting or luminescent material, the Greek word 'phosphor' is usually used and it means 'light bearer' [1]. A phosphor emits energy from an excited electron as light, and the excitation of the electron is triggered by absorption of energy from one of the external excitation sources discussed above. An excited electron occupies a quantum state whose energy is above the minimum energy ground state. In semiconductors and insulators, the electronic ground state is commonly referred to as electrons in the valence band, which is completely filled with these electrons. The excited quantum state often lies in the conduction band, which is empty and separated from the valence band by gap, E_g. Therefore, unlike metallic materials, a small continuous change in electron energy within the band is not possible. Instead, a minimum energy equal to the band gap energy is necessary to excite an electron in semiconductors and insulators, and the energy released by de-excitation is often nearly equal to the band gap. The band gap of semiconductor material is such that at room temperature, very

few electrons are promoted from the valence band to the conduction band, leaving holes in the valence band. In general, luminescence emission is explained by the transfer of energy from radiation to the electrons of the solid, thus exciting the electrons from a ground state to an excited state. The emission of a luminescent photon takes place when an excited electron returns to a lower energy state.

An electron excited to an upper energy level can return to the ground state by re-emitting a photon of the same energy as was absorbed. This phenomenon is called resonance fluorescence. Depending on the presence of other metastable states relative to the excited state energy level, emission of a photon of lower energy (Stoke's shift) or higher energy (anti-Stoke's shift) as compared to the absorbed energy can be observed when an excited electron relaxes to the ground state [10]. The wavelength of the emitted light is characteristic of the luminescent substance and not of the incident radiation. Usually, most studies of luminescence phenomena are concerned with the emission of visible light, but other wavelengths can be emitted, such as ultraviolet or infrared.

2.2 Thermoluminescence

Pagonis et al [6] , define thermoluminescence as the emission of light from a semiconductor or an insulator when it is heated, due to the previous absorption of energy from irradiation. Thus, typically thermoluminescence requires that a material must be an insulator or a semiconductor and must have been previously exposed to an irradiation source such as beta or gamma irradiation before being heated at a controlled rate to produce luminescence. Heating a sample that has been previously irradiated, releases electrons from the traps into the conduction band from where the electrons then have some probability to recombine with a hole at a recombination centre and emit light at certain wavelengths. The graph of the amount of light emitted during the TL process as a function of the sample temperature is known as a "TL glow curve." The typical glow curve contains one or more glow peaks. Each peak gives information about each trap level and its occupation state, etc in the TL material. The glow peak is analyzed by an empirical method in which a parameter called the order of kinetics is introduced'. TL has proved useful for the study of lattice defects which act as charge traps for electrons and holes, besides its application in radiation dosimetry and in archaeological and geological dating.

Figure 2.3 is the OTOR model , aligning with the singular emission band observed during the peak I temperature range. a recombination center is introduced at (N_h, n_h) to account for the emission band at 420 nm, and (N,n) is identified as the center responsible for peak I in the TL curve.

The trap is characterized by total concentration N in the crystal and by instantaneous electron occupancy

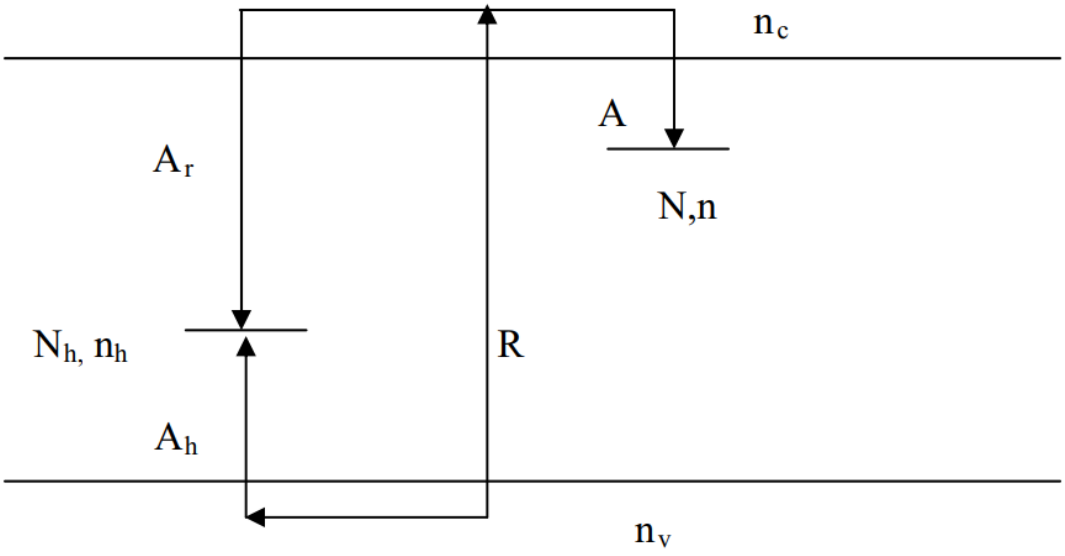

Figure 2.3: The filling of peak I trap during crystal irradiation

$n(t)$. The recombination center has instantaneous hole occupancy $n_h(t)$ and total concentration Nh in the crystal. The functions $n_c(t)$ and $n_v(t)$ represent the instantaneous concentrations of free electrons in the conduction band and free holes in the valence band correspondingly. The equations describing the rate of change of the functions $n(t)$, $n_h(t)$, $n_c(t)$, and $n_v(t)$ during the irradiation process are;

$$\frac{dn(t)}{dt} = A(N-n)n_c \tag{2.1a}$$

$$\frac{dn_v(t)}{dt} = R - A_h(N_h - n_h)n_v \tag{2.1b}$$

$$\frac{dn_h(t)}{dt} = A_h(N_h - n_h)n_v - A_r n_h n_c \tag{2.1c}$$

$$\frac{dn_c(t)}{dt} = n_h'(t) + n_v'(t) - n'(t) \tag{2.1d}$$

The first equation expresses mathematically the fact that electrons in the conduction band can be trapped into the electron trap. The second equation describes the process by which free holes in the valence band are created at a constant rate R during the excitation, and these holes can also be trapped from the valence band into the recombination center as indicated by the term $-n_v(N_h - n_h)A_h$. The third equation expresses the fact that the concentration of holes in the recombination center is changed by either trapping electrons from the conduction band (term $-n_c n_h A_r$), or by trapping holes from the valence band (term $n_v(N_h - n_h)A_h$). The last equation expresses the conservation of total charge in the crystal, with the left-hand side being equal to the total instantaneous concentration of electrons, and the right-hand side representing the total concentration of holes in the crystal at any time t.

The parameters in the above expressions are well defined in the Table 2.1

Table 2.1: Variables and Parameters

Parameter	Description	Units
A	Transition probability coefficient of electrons into the trap	$cm^{-3}s^{-1}$
A_h	Trapping probability coefficient of holes from the valence band into the recombination	$cm^{-3}s^{-1}$
A_r	Recombination probability coefficient of electrons from the conduction band into the recombination center	$cm^{-3}s^{-1}$
n	Instantaneous concentration of electrons in the electron traps at time t	cm^{-3}
N	Total concentration of electron traps in the crystal	cm^{-3}
$(N-n)$	Instantaneous concentration of empty main traps available at time t	cm^{-3}
N_h	Instantaneous concentration of holes in the recombination center	cm^{-3}
N_c	Total concentration of holes in the crystal	Cm^{-3}
n_c	Instantaneous concentration of electrons in the conduction band	cm^{-3}
n_v	Instantaneous concentration of holes in the valence band	cm^{-3}
R	Constant rate of production of electron-hole pairs	$cm^{-3}s^{-1}$

Equation 2.2 describes the dynamic nature of the thermoluminescent process during a readout stage, where n represents the concentration of trapped charge carriers(m^{-3}), s denotes attempt-to-escape frequency (s^{-1}), β is linear heating factor (K/s), k is a Boltzmann's Constant (eVK^{-1}), T is absolute temperature (K) , and E signifies the activation energy or trap depth (eV) associated with Peak I.

$$I(t) = -\frac{dn}{dt} = nse^{-\frac{E}{kT}} \tag{2.2}$$

This differential equation explains the dynamic nature of the thermoluminescent process, providing a mathematical foundation for understanding the evolution of charge carriers with respect to temperature.

2.3 Kinetic analysis

Kinetic analysis is the analysis of a thermoluminescence glow curve in order to determine physical parameters of the traps and establish the kinetics of the charge-carrier transfer between them [11]. There are several methods that can be used in order to extract relevant information from the TL glow curve. This section describes one of the methods of kinetic analysis that was particularly useful in this study

2.3.1 Peak shape method

The peak shape method can be used to evaluate E, s, and b. This method is based on the geometrical shape of a glow peak. First-order glow peaks are asymmetrical, while second-order peaks are nearly symmetrical in shape. E, s, and b are calculated using three parameters τ, δ, and ω shown in Figure 2.4.

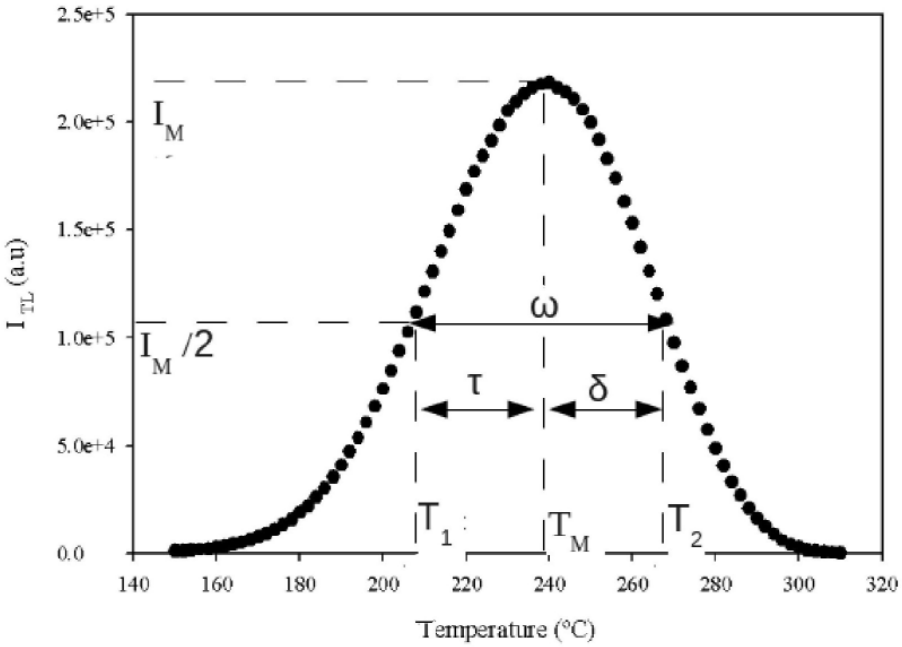

Figure 2.4: Three TL parameters τ, δ and ω used to evaluate E, s and b in a peak shape [11] method

$$\tau = T_M - T_1 \tag{2.3}$$

$$\delta = T_2 - T_M \tag{2.4}$$

$$\omega = T_2 - T_1 \tag{2.5}$$

where τ is the low-temperature half-width of a peak, δ is the half-width at high temperature, and ω is the total half-intensity width. T_1 and T_2 are low and high temperatures corresponding to half-maximum intensity, respectively. TM is the temperature at maximum intensity [11, 12]. The kinetic order b is a monotonic function of the geometrical or symmetrical factor written as

$$\mu_g = \frac{\delta}{\omega} \tag{2.6}$$

Symmetry properties of a peak are used to distinguish between first and second-order kinetics. For a first-order peak ($b = 1$), $\mu_g = 0.42$, and for second-order ($b = 2$), $\mu_g = 0.52$.

2.4 α-Al_2O_3:C

α-Al_2O_3:C is a well-known ultra-sensitive thermoluminescence and optically stimulated luminescence dosimeter (TLD/OSLD) [13], due to its ability to detect and measure ultraviolet (UV) and ionizing radiation. The doping by carbon has been found to introduce a large number of oxygen vacancies, which in turn lead to the formation of F and F^+ centers that are responsible for radiation sensitivity of Al_2O_3:C [14]. The material is grown from the melt in a reducing atmosphere of graphite at high temperatures of about 2050°C [15] and then cooled rapidly to room temperature. An F-centre is formed when an oxygen vacancy is filled with two electrons, whereas an F^+ centre is formed when an oxygen vacancy is filled with one electron.

α-Al_2O_3:C has desirable dosimetric material characteristics such as high optical, chemical, and thermal stability under irradiation [16]. Besides, it has a low-dose threshold, saturates at high doses, has a large band gap, and good optical transparency which make it suitable for dosimetric applications [17, 18]. For example, its very low-dose threshold ($\sim 10^{-6}$ Gy) has made α-Al_2O_3:C applicable to low dose dosimetry in environmental monitoring as well as in personal, medical, and accidental dosimetry [17]. By 1993, α-Al_2O_3:C was already being used for radiation monitoring in personal and environmental dosimetry in many parts of the world [16]. Its high sensitivity also makes it an appropriate material for use in space dosimetry, nuclear tracking, and security applications. A glow curve of α-Al_2O_3, generally, shows three peaks; the main dosimetric peak of high intensity (peak II) and the other two peaks of lower intensity called secondary glow peaks (peaks I and III).

Previous studies on TL in various materials have frequently employed experimental techniques to analyze TL peaks. For instance, in his research, Seneza [19] conducted kinetic analysis on TL from secondary peaks. The results indicated that the activation energy for peak I is 0.7 eV, while that for peak III is 1.2 eV. The frequency factor, which represents the frequency at which an electron attempts to escape a trap, was found to be within the range of the Debye vibration frequency $10^{12} - 10^{14}\,s^{-1}$. Consistency in the values of activation energy was observed across different methods employed. Peak I demonstrated first-order kinetics, as confirmed by the TM-Tstop method. Notably, a linear dependence of TL from peak I on dose was observed across various doses ranging from 0.5 to 2.5 Gy. Additionally, the peak position for peak I remained independent of dose, further confirming its first-order kinetics. Chithambo [20] reported that the peak-temperature of each of the secondary glow peaks was essentially constant with dose, whereas that of the main peak decreased with irradiation. The dose response for the three peaks was similar except for sublinear growth in the higher temperature peak at low dose values. Nyirenda [2] discussed that Peak I shows a sublinear dose response at doses ranging from 0.1

Gy to 10 Gy and then seems to saturate at doses above 10 Gy. The peak position of peak I seems to be stable with dose. As opposed to peak I, the dose response for peak III grows from linear from 0.1 Gy to 10 Gy to supralinear at high doses. The peak position of peak III is almost stable beyond 1 Gy of beta irradiation.

Chapter 3

Materials and Methods

This chapter covers the systematic methodology employed to simulate the thermoluminescent behavior of Peak I in carbon-doped aluminum oxide.

3.1 Materials

The information synthesis draws from an extensive array of sources including published articles, books, theses, manuscripts, and dissertations. To enhance the efficiency of data analysis and manipulation, Mathematica 13.2 (Wolfram Research) software is used. Mathematica is renowned for its user-friendly interface and powerful capabilities in handling complex simulations. It also emerges as a tool of choice due to its versatile capabilities and minimal coding requirements.

3.2 Methodology

3.2.1 Kinetic Model Equations and Model Parameters

The model applied in this study is based on the one-trap-one-recombination center (OTOR) model 2.3 of thermoluminescence. OTOR model assumes the existence of two kinds of localized states. One of the two states behaves as an electron trap and the other, as a hole trap (or a recombination center)[21].

Nyirenda's research [22] discusses TL spectra plots at different temperature ranges. This study concentrates on the temperature span of $30^{\circ}\mathrm{C} - 80^{\circ}\mathrm{C}$ since this is where peak I manifests accompanied by an emission band centered at 420 nm.

In this investigation, key parameters were defined using published numerical values. The parameters used during the irradiation stage are as follows: $N = 10^{15}\,\mathrm{cm}^{-3}$, $N_h = 3 \times 10^{14}\,\mathrm{cm}^{-3}$, $R = 10^{14}\,\mathrm{cm}^{-3}\,\mathrm{s}^{-1}$, $A = 10^{-17}\,\mathrm{cm}^{3}\,\mathrm{s}^{-1}$, $A_r = 10^{-13}\,\mathrm{cm}^{3}\,\mathrm{s}^{-1}$, and $A_h = 10^{-15}\,\mathrm{cm}^{3}\,\mathrm{s}^{-1}$. These set of numerical values for the parameters are based on the model by Pagonis, et al [4].

At $t = 0$, $n(0) = n_h(0) = n_c(0) = n_v(0) = 0$. R was varied to allow for a comprehensive examination of the temporal behavior of $n(t)$, $n_h(t)$, $n_v(t)$, and $n_c(t)$. Modifying R, allows for the understanding of the dynamic relationships among these parameters hence providing accurate in the TL process during irradiation.

The simulation also employs a first-order kinetics model represented by the differential equation 2.2 as a readout stage. Informed by Seneza's findings, we fix the activation energy at 0.7eV for Peak I in the simulations and then the parameters such as initial concentration, n_o, and heating rate,β were adjusted to have an in-depth understanding of how variations in these parameters influence the simulated behavior of the glow curve by doing peak analysis.

3.2.2 Model Validation

To ensure the reliability of our simulation results were compared against results from existing literature and where significant differences existed between the simulated results and experimental ones, the parameters were varied to achieve resemblance between the simulated behaviour and the experimental observed behaviour.

Chapter 4

Results and Discussion

This chapter presents the results and discussions of the results obtained from the various simulations during the investigations.

4.1 Simulation of peak I TL process using OTOR model.

4.1.1 Irradiation stage

In this study, in order to investigate how certain traps get filled during the irradiation process , equation 2.1 was employed. Key parameters were defined using published numerical values and R was varied to allow for exploring the behaviour of $n(t)$. $n_h(t)$, $n_v(t)$, and n_c in a total irradiation of 10 s. In figure 4.1, panel (a) shows the plot of the instantaneous concentration of electrons in the electron trap as a function of time. Similarly, panel (b) shows the plot of the the instantaneous concentration of electrons in the conduction band as a function of time. Instantaneous concentration of holes in the recombination center as a function of time is shown in panel (c) whereas panel (d) shows the plot instantaneous concentration of holes in the valence band as a function of time. Panel (a) shows that with time the instantaneous concentration of electrons in the electron trap is increasing. As shown in panel (b), the instantaneous concentration of electrons in the conduction band is increasing then it saturates. Instantaneous concentration of holes in the recombination center increases with time from 0 to 1.7 s then starts becoming saturated thereafter as shown in panel (c). Similarly, panel (d) behaves the same way as panel (b) that the instantaneous concentration of holes in the valence band is increasing then it becomes saturated.

From this irradiation simulation, it is observed that as time goes on, the concentrations of holes, and

electrons in the bands increase. This suggests that more holes and electrons are accumulating in the material's valence and conduction bands.

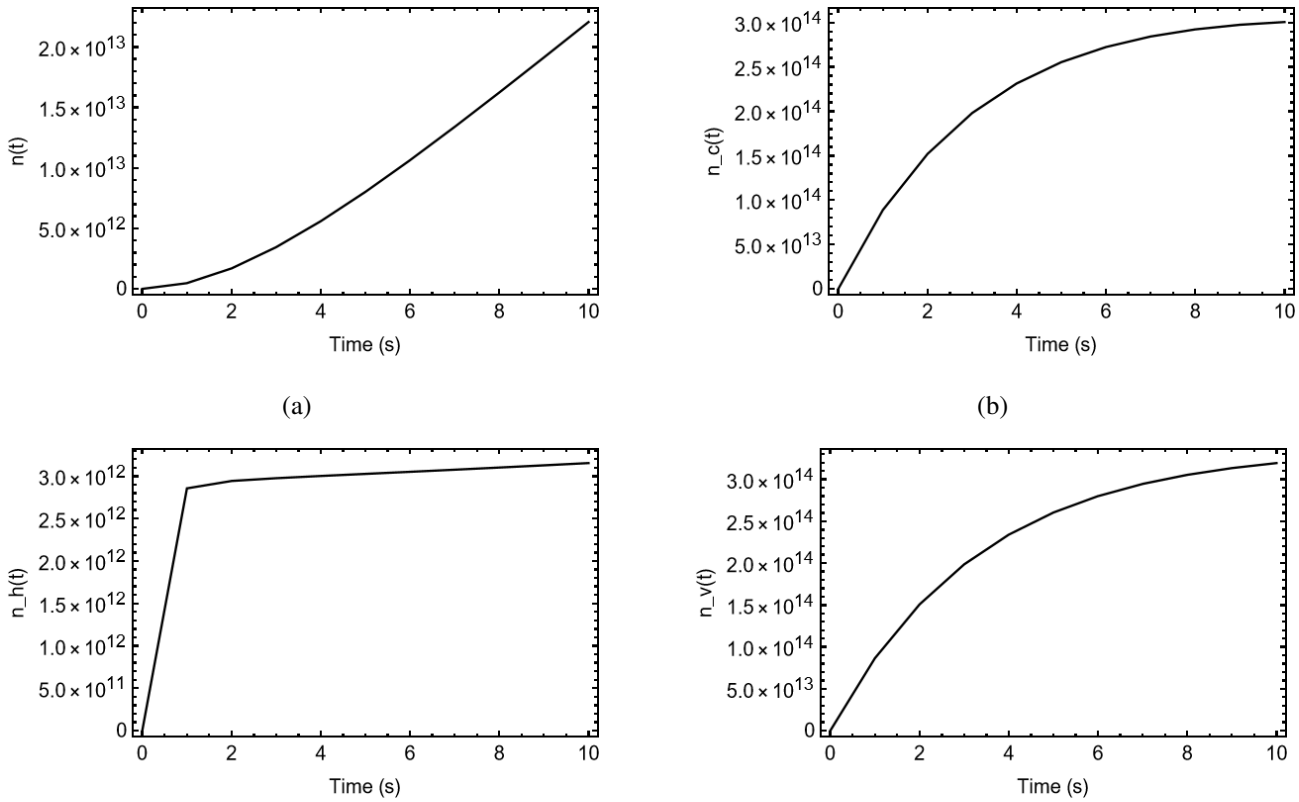

Figure 4.1: Variations of $n(t)$, $n_h(t)$, $n_c(t)$, and $n_v(t)$ during irradiation.

As R gets bigger, reaching a point around 10^{17} , the total number of electron-hole pairs (that's $n(t)$ and the $n_h(t)$) get saturated.

4.1.2 Readout stage

4.1.2.1 The effects of dose on TL glow curve

To study the behavior of Peak I in α-Al_2O_3:C, equation 2.2 was employed. The values of other parameters involved in equation 2.2 are as follows: $s = 10^{10}\,s^{-1}; n_1 = 1\times10^{10}\,m^{-3}; n_2 = 2\times10^{10}\,m^{-3}; n_3 = 3\times10^{10}\,m^{-3}; n_4 = 4\times10^{10}\,m^{-3}; n_5 = 5\times10^{10}\,m^{-3}; k = 8.617\times10^{-5}\,eV/K; E = 0.7\,eV; \beta = 1K/s$. Figure 4.2 shows how TL varies with the dose. As seen in Figure 4.2, peak intensity increases with increasing dose.

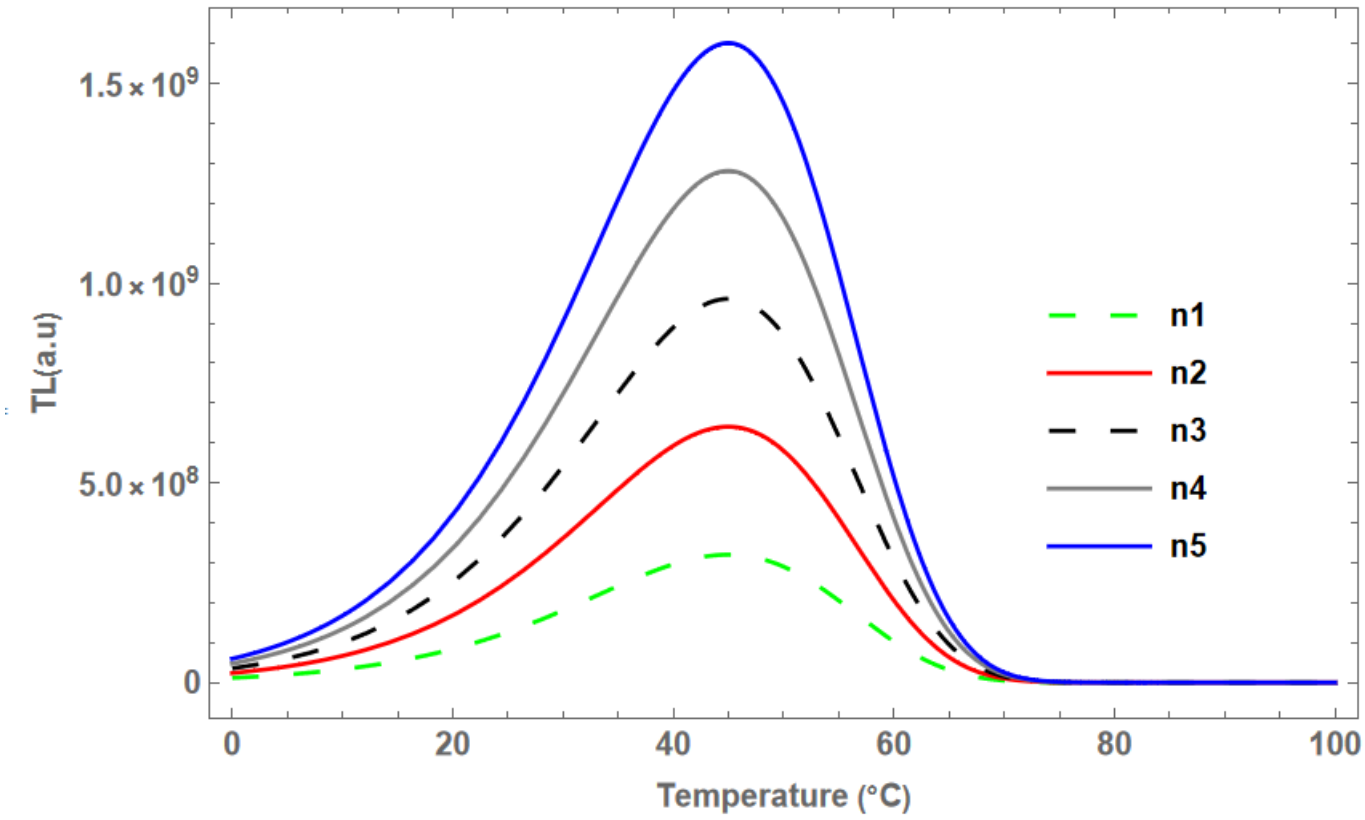

Figure 4.2: Plots of TL glow curves for various dose

The subsequent analyses are derived from figure 4.2. Figure 4.3 shows the plot of the maximum peak position T_M as a function of dose. Figure 4.4 shows the plot of maximum peak intensity as a function of dose. Similarly, Figure 4.5 shows the plot of FWHM as a function of dose whereas figure 4.6 shows the plot of the geometrical shape factor as a function of dose.

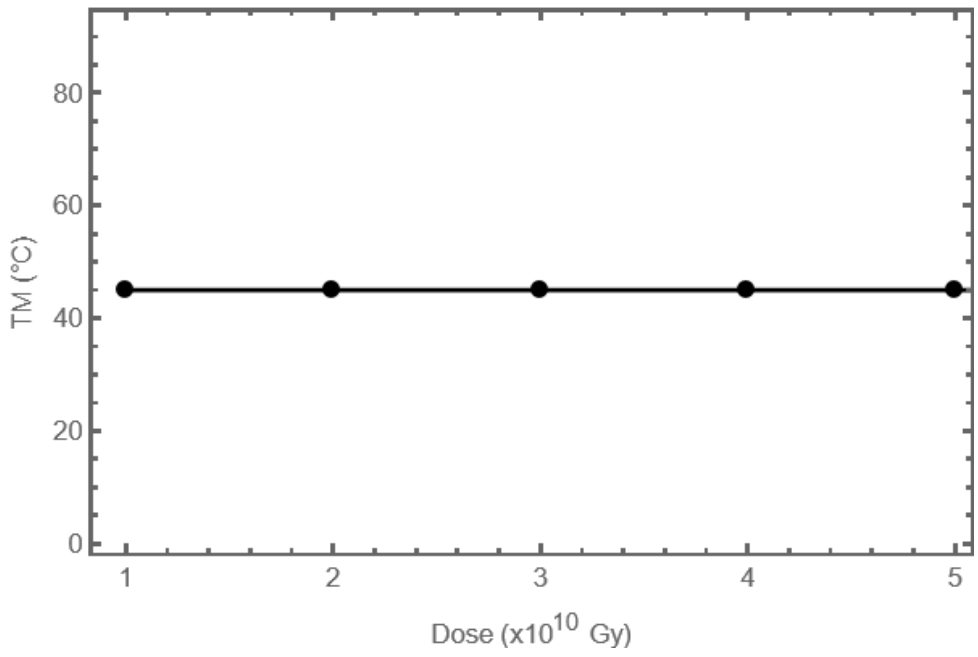

Figure 4.3: The dependence of the maximum peak position T_M on the dose

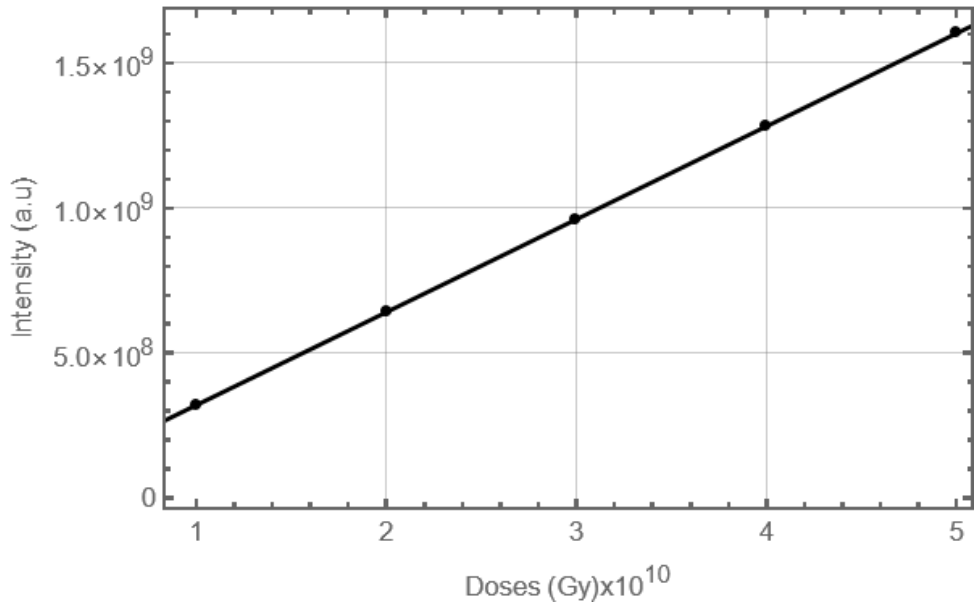

Figure 4.4: Plot of maximum peak intensity against dose

Figure4.3 shows how the maximum peak position T_M of the peak I, varies with the doses. The results show that the peak position does not change with dose. This is consistent with first-order kinetics. Seneza [19] also reached at the same conclusion that the peak position of the peak I does not change with dose. Similarly, Nyirenda [2] made the same conclusion that the peak position of peak I seems to be stable with dose. Therefore, it is clear that based on the behaviour of maximum peak position with dose peak I follows first-order kinetics. Figure 4.4 shows how the Maximum peak intensity I_M of peak I varies with the doses. It can be noted that increasing the dose also increases the maximum peak

intensity. This aligns with first-order behaviour of thermoluminescence. Ayta [23] made a conclusion that the maaximum peak intensity with dose behaves linearly for the main peak in Li_2O–B_2O_3–Al_2O_3 glass system doped with CaF_2 and Mn. Hence, it is clear that based on the maximum peak position with dose peak I suggests first order kinetics. Figure 4.5 shows how the FWHM varies with the dose and Figure 4.6 shows geometrical shape factor against dose. Furthermore, the results shows that FWHM and geometrical shape factor are both independent of dose.

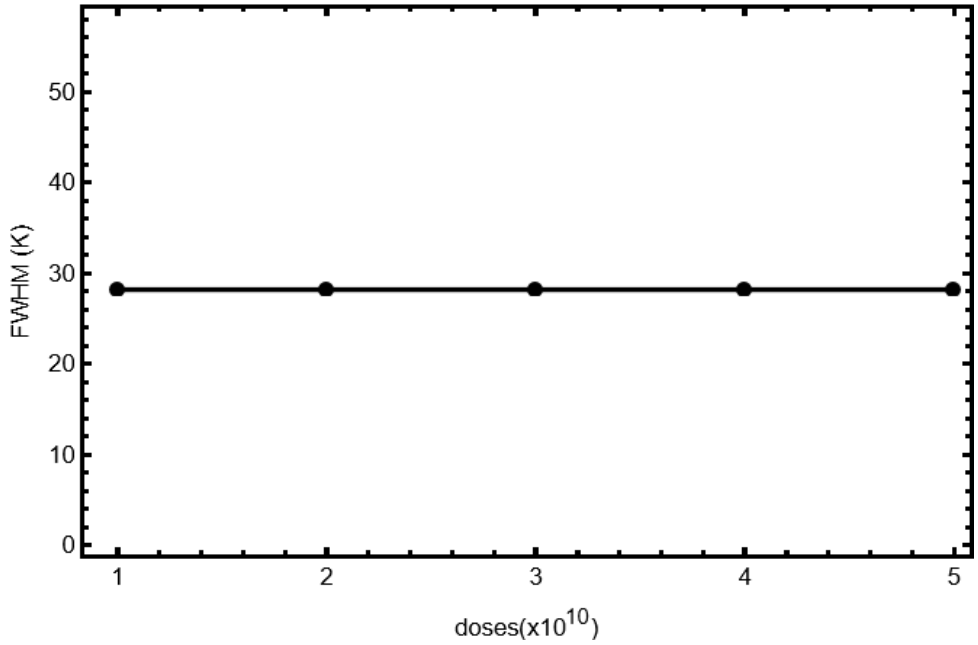

Figure 4.5: Full with Half Maximum (FWHM) versus dose

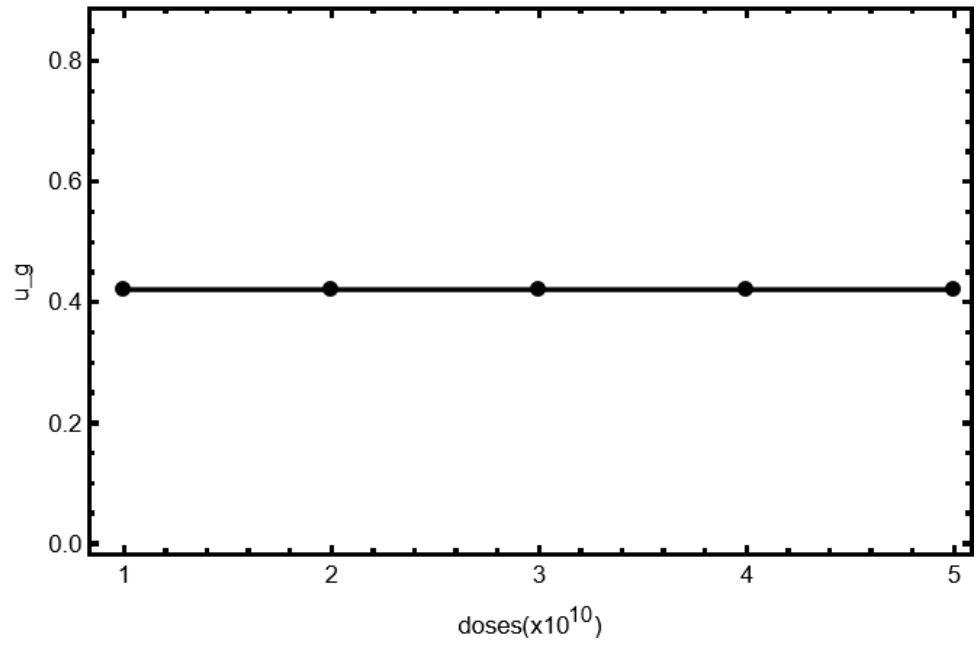

Figure 4.6: Geometrical shape factor versus dose

From the dose responses analysis, it appears that the maximum peak position is proportional to doses due to the accumulation of more trapped charge carriers generated by ionization radiation. As the dose increases, more charge carriers get trapped by the traps within the material while storing additional energy. Therefore, during readout stored energy is released as light, resulting in higher peak intensity. FWHM as a function of dose behaves in that way as at this point recombination centers are saturated and any further increase in dose may not lead to a significant change in the FWHM and geometrical shape factor with dose varies linearly may be due to the material's trapping sites become full at higher doses, so any additional doses have less impact on the glow peak's shape.

From the given figure 4.2 for a TL glow peak I, three temperatures required for Chen's peak shape equations were estimated. The quantities for each glow curve were calculated as follows:

$$\begin{aligned}
\tau &= (317.98 - 301.23)\,\mathrm{K} = 16.75\,\mathrm{K}, \\
\delta &= (330.16 - 317.98)\,\mathrm{K} = 12.18\,\mathrm{K}, \\
\omega &= (330.16 - 301.23)\,\mathrm{K} = 28.93\,\mathrm{K}, \\
\mu_g &= \frac{\delta}{\omega} = \frac{12.18}{28.93} \approx 0.4210.
\end{aligned}$$

The average value of the geometrical shape factor μ_g was calculated as $\mu_g = 0.4210162461$ for a variety doses. This finding seems to exhibit first-order behaviour for a broad range of doses, aligning with theoretical expectations, where the first-order peaks have $\mu_g = 0.42$. This consistency with theoretical predictions supports the idea that Peak I follows first-order kinetics. additionally, the experimental results obtained by Seneza [19] reported a similar behaviour in his study.

4.1.2.2 The effects of heating rate on the TL of peak I

In the investigation of Peak I behavior in carbon-doped aluminum oxide, equation 2.2 was employed to model the thermal behavior. The values assigned to these parameters are as follows: $s = 10^{10}\,\mathrm{s}^{-1}$; $n_1 = 1 \times 10^{10}\,\mathrm{m}^{-3}$; $k = 8.617 \times 10^{-5}\,\mathrm{eV/K}$; $E = 0.7\,\mathrm{eV}$; $\beta = 0.1\,\mathrm{K/s}$; $\beta = 0.2\,\mathrm{K/s}$; $\beta = 2\,\mathrm{K/s}$; $\beta = 4\,\mathrm{K/s}$. Figure 4.7 shows the variation of Thermoluminescence (TL) with different heating rates.

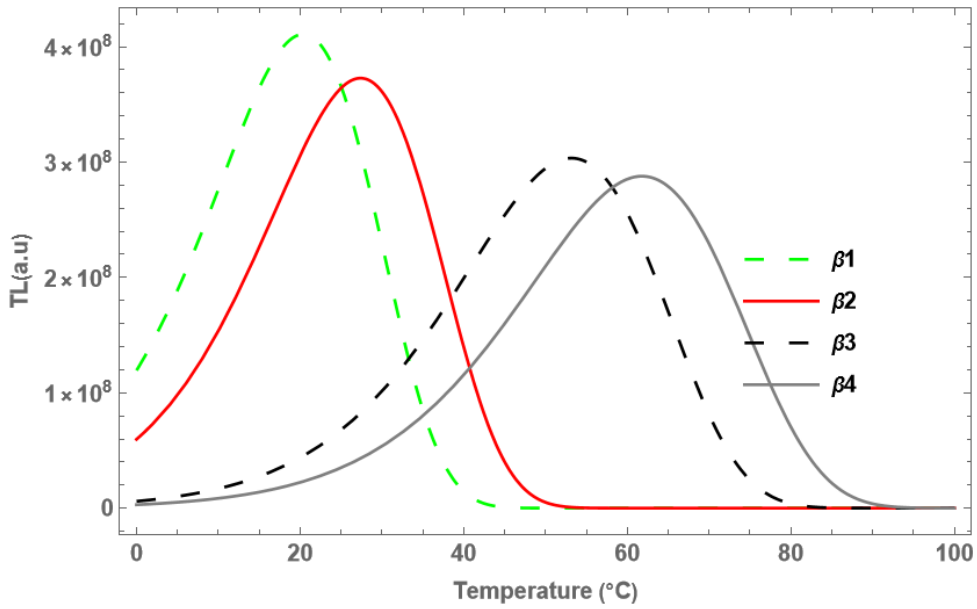

Figure 4.7: Plots of TL glow curves at different heating rates

Figure 4.7 shows the graph of the maximum peak intensity as a function of Temperature for different heating rates. From figure 4.7 It is clear that when the heating rate increases, the maximum peak intensity decreases, while the peak temperature shift towards higher values with an increase of the heating rate. For instance, the maximum intensity is $I_{M1} = 4.10794 \times 10^8$ counts/s for $\beta_1 = 0.1\,\mathrm{Ks}^{-1}$ and $I_{M4} = 2.8773 \times 10^8$ counts/s for $\beta_4 = 4\,\mathrm{Ks}^{-1}$. Further, Figure 4.7 shows that the width of the glow curves become broader and broader with an increase in the heating rate. It is well known that the size of the width is associated with the dissipation (scattering) in a material medium [24]. Hence, it means that as the heating rate increases, the scattering in the system is also increased which is reflected via an increased broadening of the width of the glowcurve. These two indicators are shown in Figure 4.7 as a direct result of increasing the heating rate: (i) the maximum peak position is shifted towered the high-temperature values and (ii) the maximum peak intensity decreases with increasing the heating rate, may be explained by the thermal quenching effect [25, 26]. The change of maximum peak intensity with heating rate as reported here was also observed by Nanjundaswamy [27] who found that at low heating rates the TL peak may appear in a range where thermal quenching is minimal, whereas at high heating rates the peak temperature may be such that thermal quenching is strong. Indeed, the observed effect of the heating rate on the TL glow curves of peak I is expected, and the material is obeying the theoretical predictions. This is in line with the typical behaviour in first-order kinetics.

Figure 4.8 shows how the maximum peak intensity of peak I , varies with the heating rate. Figure 4.9 shows how FWHM varies with the heating rate and figure 4.10 show how geometrical shape factor varies with the heating rate. Similarly, figure 4.11 shows how the maximum peak position varies with

heating rate. All peak heights were quoted in arbitrary units. As shown in figure 4.8, the maximum peak intensity decreases with increasing heating rate. This is consistent with the first-order behavior of TL. Seneza [19] also reached at the same conclusion that the maximum peak intensity of peak I decreases with the heating rate. it is clear that based on the behavior of maximum peak intensity of heating rate peak I follows first-order kinetics.

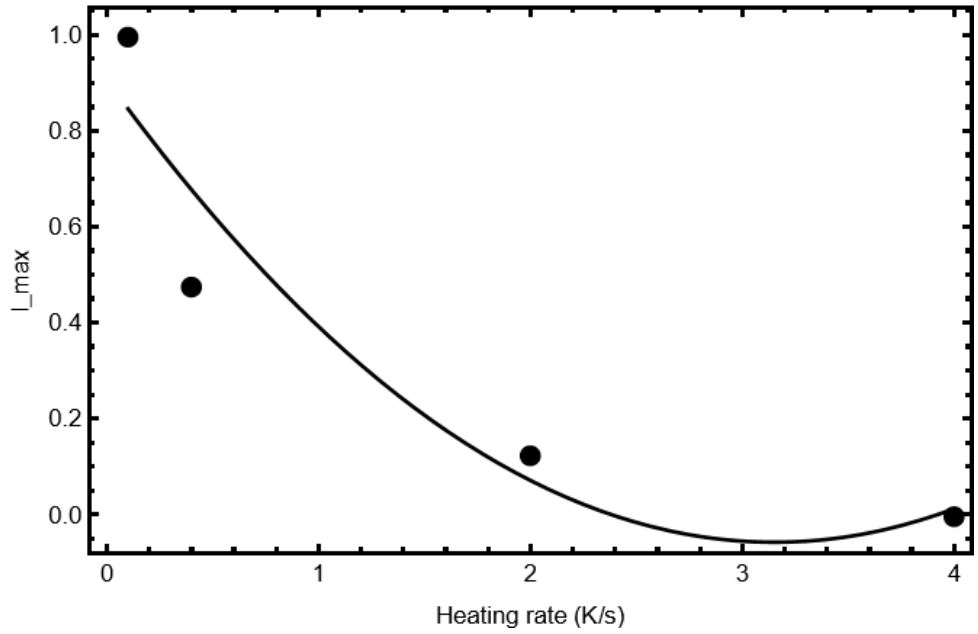

Figure 4.8: Plot of maximum intensity against the heating rate

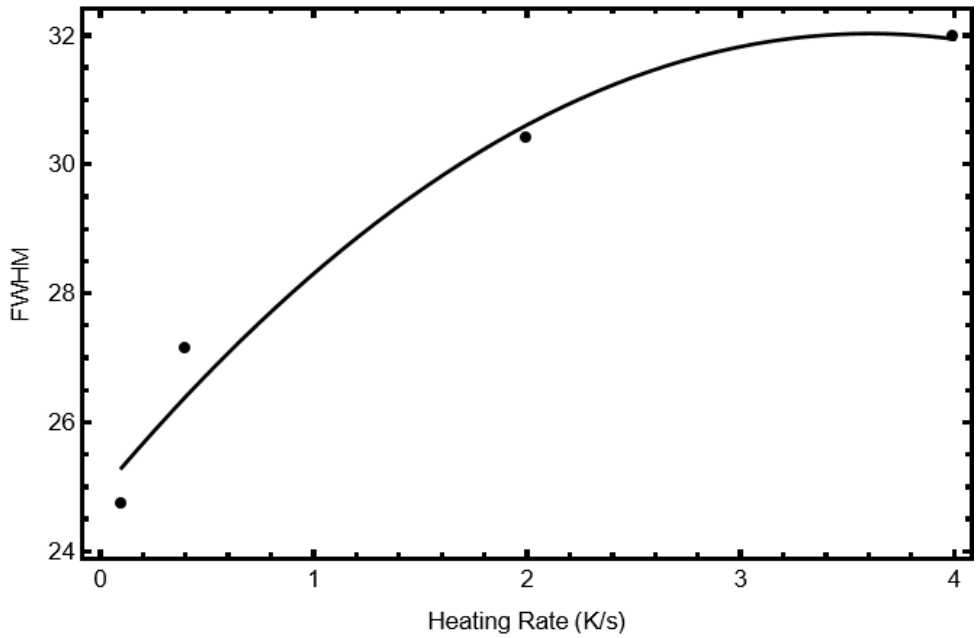

Figure 4.9: Full Width at Half Maximum (FWHM) of peak I at different heating rate

Moving on to Figure 4.9, it shows the variation in the Full Width at Half Maximum (FWHM) with

the heating rate. The results show that FWHM increases with increasing heating rate until into the saturation region where it appears to be almost constant with heating rate. This sheds light on how the spectral width evolves in response to different rates of heating. This aligns with first-order behaviour of TL. Similarly, Figure 4.10 shows that the geometric shape Factor of peak I slightly increases and the saturate. Finally, Figure4.11 shows that with an increase in heating rate, the maximum peak position of peak I increase between 0 K/s and 3 K/s, and above (3 K/s) it saturates. This is consistent with the first-order behaviour. This behaviour of dynamic throughput is similar to that reported by Furetta [28]. The same behaviour was also reported in the study by Sharm[29].

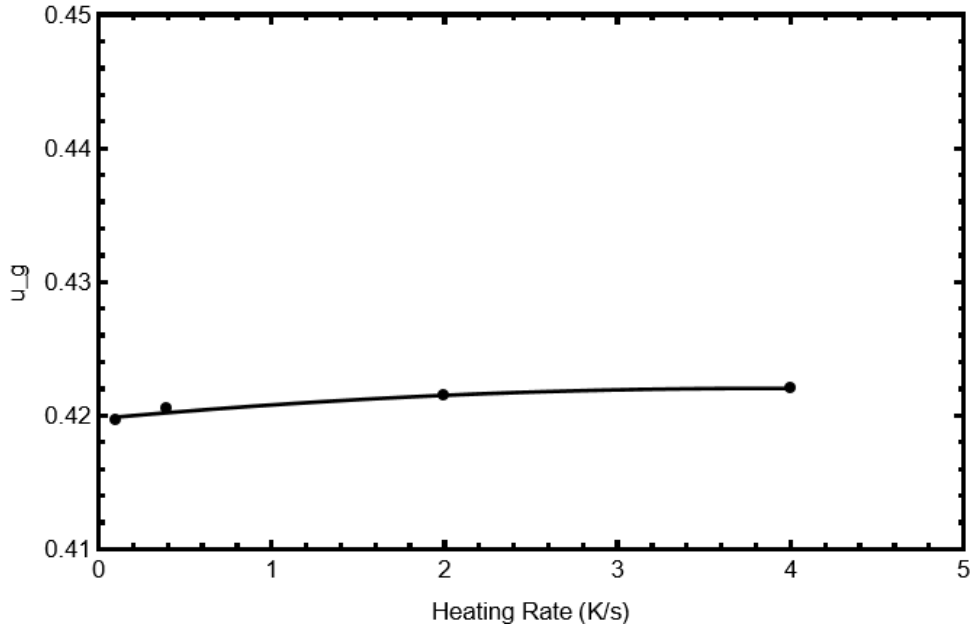

Figure 4.10: Plot of geometrical shape factor (u_g) against different heating rate

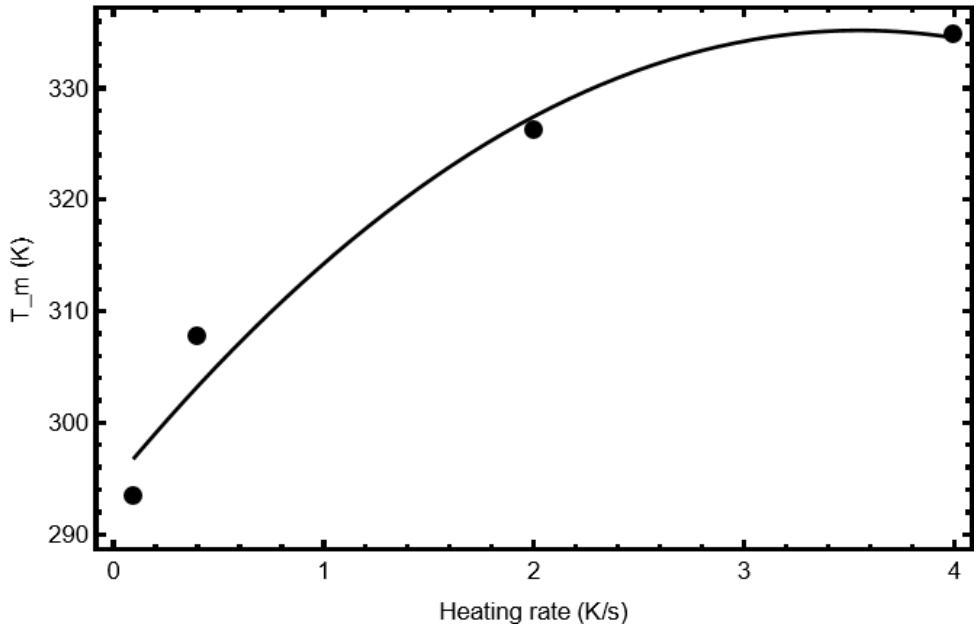

Figure 4.11: Plot of maximum peak position (T_M) against heating rates.

Figure 4.11 shows the dependence of peak position on the heating rate for peak I. The peak position of the peak I shifts to higher temperatures with increasing heating rate. The shifting of the peak position to higher temperature is a mathematical consequence due to the dependence of peak position on heating rate for first-order kinetics i.e:

$$\beta = \frac{skT_M^2}{E} \exp\left(\frac{E}{kT_M}\right) \tag{4.1}$$

which shows that β is an increasing function of T_M assuming that E and s are constant. This means that as the heating rate increases, the peak must shift to higher temperatures.

Chapter 5

Conclusions

In this work, we studied the TL phenomena of peak I in α-Al_2O_3:C by employing OTOR model. According to this study, from the investigation carried out on peak I, it can be concluded that the simulated TL behaviour agrees well with the experimental behaviour and that both simulated and experimental behaviour of peak I follows first-order kinetics

For TL simulations carried out at different heating rate, it has been shown that the maximum peak position of peak I decreases with heating rate. The decrease in maximum peak position is due to thermal quenching. We have also seen that with increasing heating rate, the FWHM becomes broader and broader. it is well known that the size of the width is associated with scattering in the material medium. In addition, with increasing heating rate, the maximum peak positions of all the peaks, shift towards higher temperatures, because of the direct mathematical relationship that exists between the heating rate and the peak position. Simulations were also carried out at different doses. The result has shown that the maximum peak position , FWHM ,and geometrical shape factor are all independent of dose.

References

[1] McKeever S.W.S. Thermoluminescence of solids, cambridge university press, cambridge. 1985.

[2] Angel Newton Nyirenda. Mechanisms of luminescence in α-al$_2$o$_3$: Investigations using time-resolved optical stimulation and thermoluminescence techniques. *Rhodes University, South Africa*, 2012.

[3] A Nyirenda and M Chithambo. Kinetic analysis of the main glow peak of α-al2o3: C exposed to high irradiation dose. *Journal of Nuclear Sciences*, 2(2):23–30, 2015.

[4] V Pagonis, R Chen, and JL Lawless. A quantitative kinetic model for al2o3: C: Tl response to ionizing radiation. *Radiation Measurements*, 42(2):198–204, 2007.

[5] Stephen WS McKeever. *Thermoluminescence of solids*, volume 3. Cambridge University Press, 1985.

[6] Vasilis Pagonis, George Kitis, and Claudio Furetta. *Numerical and practical exercises in thermoluminescence*. Springer Science & Business Media, 2006.

[7] Miho Hatanaka and Satoshi Yabushita. Theoretical study on the f- f transition intensities of lanthanide trihalide systems. *The Journal of Physical Chemistry A*, 113(45):12615–12625, 2009.

[8] Hikaru Unesaki, Takuji Kato, Seiji Watase, Kimihiro Matsukawa, and Kensuke Naka. Polymorph control of luminescence properties in molecular crystals of a platinum and organoarsenic complex and formation of stable one-dimensional nanochannel. *Inorganic Chemistry*, 53(16):8270–8277, 2014.

[9] C Furetta, S Guzman, B Ruiz, and E Cruz-Zaragoza. Retraction notice to "the initial rise method extended to multiple trapping levels in thermoluminescent materials"[appl. radiat. isot. 69 (2011), 346–349]. *Applied Radiation and Isotopes*, 9(69):1322, 2011.

[10] Semiconductor Nanocrystal Quantum Dots. Synthesis, assembly. *Spectroscopy and Applications.(Springer, 2010)*, 2008.

[11] Yoram Kirsh. Kinetic analysis of thermoluminescence. *physica status solidi (a)*, 129(1):15–48, 1992.

[12] Reuven Chen and Stephen WS McKeever. *Theory of thermoluminescence and related phenomena*. World Scientific, 1997.

[13] DR Mishra, MS Kulkarni, KP Muthe, C Thinaharan, M Roy, SK Kulshreshtha, S Kannan, BC Bhatt, SK Gupta, and DN Sharma. Luminescence properties of α-al2o3: C crystal with intense low temperature tl peak. *Radiation measurements*, 42(2):170–176, 2007.

[14] KP Muthe, MS Kulkarni, NS Rawat, DR Mishra, BC Bhatt, Ajay Singh, and SK Gupta. Melt processing of alumina in graphite ambient for dosimetric applications. *Journal of luminescence*, 128(3):445–450, 2008.

[15] SWS McKeever, M Moscovitch, and PD Townsend. Thermoluminescence dosimetry materials: Properties and uses nuclear technology publishing. *Ashford, Kent, UK ISBN*, pages 1–870965, 1995.

[16] MS Akselrod, VS Kortov, and EA Gorelova. Preparation and properties of alpha-al2o3: C. *Radiation Protection Dosimetry*, 47(1-4):159–164, 1993.

[17] KP Muthe, SK Gupta, JV Yakhmi, MS Kulkarni, DR Mishra, A Soni, and DN Sharma. Development of α-al 2 o 3: C phosphor for optically stimulated luminescence based personnel dosimetry. In *Proceedings of international conference on peaceful uses of atomic energy-2009. V. 2*, 2009.

[18] Yuri F Zhukovskii, Eugene A Kotomin, Robert A Evarestov, and Donald E Ellis. Periodic models in quantum chemical simulations of f centers in crystalline metal oxides. *International Journal of Quantum Chemistry*, 107(14):2956–2985, 2007.

[19] Cleophace Seneza. Thermoluminescence of secondary glow peaks in carbon-doped aluminium oxide. 2014.

[20] Makaiko L Chithambo. Concerning secondary thermoluminescence peaks in α-al2o3: C. *South African journal of science*, 100(11):524–527, 2004.

[21] A Halperin and AA Braner. Evaluation of thermal activation energies from glow curves. *Physical Review*, 117(2):408, 1960.

[22] Angel N Nyirenda and Makaiko L Chithambo. Spectral study of radioluminescence in carbon-doped aluminium oxide. *Radiation Measurements*, 120:89–95, 2018.

[23] WEF Ayta, VA Silva, and NO Dantas. Thermoluminescent properties of a li2o–b2o3–al2o3 glass system doped with caf2 and mn. *Journal of luminescence*, 130(6):1032–1035, 2010.

[24] Challa SSR Kumar. *UV-VIS and photoluminescence spectroscopy for nanomaterials characterization*. Springer, 2013.

[25] PR González, C Furetta, E Cruz-Zaragoza, and J Azorín. Heating rate effects on thermoluminescence of baso 4: Eu+ ptfe prepared at inin-mexico. *Modern Physics Letters B*, 24(08):717–726, 2010.

[26] Jumpei Ueda, Pieter Dorenbos, Adrie JJ Bos, Andries Meijerink, and Setsuhisa Tanabe. Insight into the thermal quenching mechanism for y3al5o12: Ce3+ through thermoluminescence excitation spectroscopy. *The Journal of Physical Chemistry C*, 119(44):25003–25008, 2015.

[27] R Nanjundaswamy, K Lepper, and S WS McKeever. Thermal quenching of thermoluminescence in natural quartz. *Radiation protection dosimetry*, 100(1-4):305–308, 2002.

[28] Claudio Furetta and Pao-Shan Weng. *Operational thermoluminescence dosimetry*. World Scientific, 1998.

[29] Geeta Sharm, Puja Chawla, SP Lochab, and Nafa Singh. Thermoluminescence characteristics of cas: Ce nanophosphors. *Chalcogenide letters*, 6(9), 2009.

Appendix A

Appendix

MATHEMATICA CODES USED IN THE STUDY

A.1 Simulation of peak I TL process using OTOR model: irradiation stage

```
programMain := (A = 10^{-17}; Ar = 10^{-13}; Ah = 10^{-15};
   N1 = 10^15; Nh = 3*10^14;
   solveDiffeq[n10_, nh0_, nv0_, nc0_, R_, tfinal_] :=
    Module[{t},
     NDSolve[{n1'[t] == A*(N1 - n1[t])*nc[t],
       nh'[t] == -Ar*nh[t]*nc[t] + Ah*nv[t]*(Nh - nh[t]),
       nv'[t] == R - Ah*nv[t]*(Nh - nh[t]),
       nc'[t] == nh'[t] + nv'[t] - n1'[t], n1[0] == n10, nc[0] == nc0,
        nv[0] == nv0, nh[0] == nh0}, {n1, nh, nv, nc}, {t, 0, tfinal},
       MaxSteps -> 50000]];
   initValues[b_, d_] := Module[{}, n10 = Last[n1[d] /. b];
     nh0 = Last[nh[d] /. b];
     nv0 = Last[nv[d] /. b];
     nc0 = Last[nc[d] /. b];];
   (*Irradiation*)R = 10^14; tfinal9 = irrTime;
   sol9 = solveDiffeq[n10, nh0, nv0, nc0, R, tfinal9];
```

```
    );

(*-----------------------------------------------*)
tstart = 0; tend = 10; tstep = 1;
n1List1 = {}; n1List2 = {{, }};
ncList = {}; nhList = {}; nvList = {};

For[tloop = tstart , tloop <= tend , tloop += tstep , n10 = 0; nh0 = 0;
 nv0 = 0; nc0 = 0;
 irrTime = tloop;
 programMain;
 initValues[sol9 ,
  tfinal9 ];(*find values at the end of irradiation stage*)
 AppendTo[n1List1 , {tloop , n1[tloop] /. sol9[[1]]}];
 AppendTo[ncList , {tloop , nc[tloop] /. sol9[[1]]}];
 AppendTo[nhList , {tloop , nh[tloop] /. sol9[[1]]}];
 AppendTo[nvList , {tloop , nv[tloop] /. sol9[[1]]}];]

(*Plots*)
nGrp1 = ListPlot[n1List1 , PlotRange -> All , Joined -> True ,
   Frame -> True , PlotStyle -> Directive[Black , Thickness[0.005]],
   FrameStyle -> Directive[Black , Thickness[0.005]],
   PlotLabel -> "n(t) vs time (s)", ImageSize -> 300];
ncGrp2 =
  ListPlot[ncList , PlotRange -> All , Frame -> True , Joined -> True ,
   PlotStyle -> Directive[Black , Thickness[0.005]],
   FrameStyle -> Directive[Black , Thickness[0.005]],
   PlotLabel -> "n_c(t) vs time (s)", ImageSize -> 300];
nhGrp3 =
  ListPlot[nhList , PlotRange -> All , Joined -> True , Frame -> True ,
   PlotStyle -> Directive[Black , Thickness[0.005]],
   FrameStyle -> Directive[Black , Thickness[0.005]],
```

```
   PlotLabel -> "n_h(t) vs time (s)", ImageSize -> 300];
nvGrp4 =
  ListPlot[nvList, PlotRange -> All, Joined -> True, Frame -> True,
   PlotStyle -> Directive[Black, Thickness[0.005]],
   FrameStyle -> Directive[Black, Thickness[0.005]],
   PlotLabel -> "n_v(t) vs time (s)", ImageSize -> 300];
{nGrp1, ncGrp2, nhGrp3, nvGrp4}
```

A.2 The effects of dose on thermoluminescence glow curve.

```
(*This program shows the effects of dose on
thermoluminescence glow curve.The kinetic parameters for calculations
are shown in below *)
s = 10^10; n1 = 1*10^10; n2 = 2*10^10; n3 = 3*10^10; n4 =
 4*10^10; n5 = 5*10^10; k = 8.617*10^-5; E1 = 0.7; \[Beta] = 1;

TL1 = NDSolve[{n'[x] == -n[x]*s/\[Beta]*E^(-E1/(k*(273 + x))),
    n[0] == n1}, n, {x, 0, 100}];
TL2 = NDSolve[{n'[x] == -n[x]*s/\[Beta]*E^(-E1/(k*(273 + x))),
    n[0] == n2}, n, {x, 0, 100}];
TL3 = NDSolve[{n'[x] == -n[x]*s/\[Beta]*E^(-E1/(k*(273 + x))),
    n[0] == n3}, n, {x, 0, 100}];
TL4 = NDSolve[{n'[x] == -n[x]*s/\[Beta]*E^(-E1/(k*(273 + x))),
    n[0] == n4}, n, {x, 0, 100}];
TL5 = NDSolve[{n'[x] == -n[x]*s/\[Beta]*E^(-E1/(k*(273 + x))),
    n[0] == n5}, n, {x, 0, 100}];

Plot[{Evaluate[-n'[x] /. TL1],
                                        Evaluate[-n'[x] /. TL2],

  Evaluate[-n'[x] /. TL3],

  Evaluate[-n'[x] /. TL4],
                                                                \
```

```
                Evaluate[-n'[x] /. TL5]},
                                {x, 0, 100}, ImageSize -> 500,
 PlotRange -> All, Frame -> True,

 LabelStyle -> Directive[Bold, 12],
 PlotStyle -> {{Dashing[Large], Green}, Red, {Dashing[Large], Black},
   Gray, Blue},
 PlotLegends -> Placed[{"n1", "n2", "n3", "n4", "n5"}, {0.8, 0.4}]]
```

A.3 Calculating TM and IM

```
s = 10^10; n1 = 1*10^10; n2 = 2*10^10; n3 = 3*10^10; n4 =
 4*10^10; n5 = 5*10^10; k = 8.617*10^-5; E1 = 0.7; \[Beta] = 1;

TL1 = NDSolve[{n'[x] == -n[x]*s/\[Beta]*E^(-E1/(k*(273 + x))),
    n[0] == n1}, n, {x, 0, 100}];
TL2 = NDSolve[{n'[x] == -n[x]*s/\[Beta]*E^(-E1/(k*(273 + x))),
    n[0] == n2}, n, {x, 0, 100}];
TL3 = NDSolve[{n'[x] == -n[x]*s/\[Beta]*E^(-E1/(k*(273 + x))),
    n[0] == n3}, n, {x, 0, 100}];
TL4 = NDSolve[{n'[x] == -n[x]*s/\[Beta]*E^(-E1/(k*(273 + x))),
    n[0] == n4}, n, {x, 0, 100}];
TL5 = NDSolve[{n'[x] == -n[x]*s/\[Beta]*E^(-E1/(k*(273 + x))),
    n[0] == n5}, n, {x, 0, 100}];

maxIntensities = {FindMaximum[Evaluate[-n'[x] /. TL1], {x, 0, 100}],
   FindMaximum[Evaluate[-n'[x] /. TL2], {x, 0, 100}],
   FindMaximum[Evaluate[-n'[x] /. TL3], {x, 0, 100}],
   FindMaximum[Evaluate[-n'[x] /. TL4], {x, 0, 100}],
   FindMaximum[Evaluate[-n'[x] /. TL5], {x, 0, 100}]};

TableForm[maxIntensities,
 TableHeadings -> {{"n1", "n2", "n3", "n4",
```

```
    "n5"}, {"Max Intensity(IM)", "Peak Position (TM)"}}]

  Placed[{"\[Beta]1", "\[Beta]2", "\[Beta]3", "\[Beta]4"}, {.8, .4}]]
```

A.4 The effects of heating rate on the thermoluminescence glow curve.

```
    (*This program shows the effects of heating rate (\[Beta]) on the
thermoluminescence glow curve.The kinetic parameters for
calculations are shown in below *)
s = 10^10; n1 = 1*10^10; k =
 8.617*10^-5; E1 = 0.7; \[Beta]1 = .1; \[Beta]2 = .2; \[Beta]3 = 2; \
\[Beta]4 = 4;

TL1 = NDSolve[{n'[x] == -n[x]*s/\[Beta]1*E^(-E1/(k*(273 + x))),
    n[0] == n1}, n, {x, 0, 100}];
TL2 = NDSolve[{n'[x] == -n[x]*s/\[Beta]2*E^(-E1/(k*(273 + x))),
    n[0] == n1}, n, {x, 0, 100}];
TL3 = NDSolve[{n'[x] == -n[x]*s/\[Beta]3*E^(-E1/(k*(273 + x))),
    n[0] == n1}, n, {x, 0, 100}];
TL4 = NDSolve[{n'[x] == -n[x]*s/\[Beta]4*E^(-E1/(k*(273 + x))),
    n[0] == n1}, n, {x, 0, 100}];

Plot[{Evaluate[-n'[x] /. TL1], Evaluate[-n'[x] /. TL2],
  Evaluate[-n'[x] /. TL3], Evaluate[-n'[x] /. TL4]}, {x, 0, 100},
 ImageSize -> 500, PlotRange -> All, Frame -> True,
 LabelStyle -> Directive[Bold, 12],
 PlotStyle -> {{Dashing[Large], Green}, Red, {Dashing[Large], Black},
   Gray, Blue}]
```